We are IntechOpen, the world's leading publisher of Open Access books Built by scientists, for scientists

6,900
Open access books available

185,000
International authors and editors

200M
Downloads

Our authors are among the

154
Countries delivered to

TOP 1%
most cited scientists

12.2%
Contributors from top 500 universities

WEB OF SCIENCE™

Selection of our books indexed in the Book Citation Index in Web of Science™ Core Collection (BKCI)

Interested in publishing with us?
Contact book.department@intechopen.com

Numbers displayed above are based on latest data collected.
For more information visit www.intechopen.com

Chapter 5

E-ALD: Tailoring the Optoeletronic Properties of Metal Chalcogenides on Ag Single Crystals

Emanuele Salvietti, Andrea Giaccherini, Filippo Gambinossi, Maria Luisa Foresti, Maurizio Passaponti, Francesco Di Benedetto and Massimo Innocenti

Additional information is available at the end of the chapter

http://dx.doi.org/10.5772/intechopen.71014

Abstract

Technological development in nanoelectronics and solar energy devices demands nanostructured surfaces with controlled geometries and composition. Electrochemical atomic layer deposition (E-ALD) is recognized as a valid alternative to vacuum and chemical bath depositions in terms of growth control, quality and performance of semiconducting systems, such as single 2D semiconductors and multilayered materials. This chapter is specific to the E-ALD of metal chalcogenides on Ag single crystals and highlights the electrochemistry for the layer-by-layer deposition of thin films through surface limited reactions (SLRs). Also discussed herein is the theoretical framework of the under potential deposition (UPD), whose thermodynamic treatment open questions to the correct interpretation of the experimental data. Careful design of the E-ALD process allows fine control over both thickness and composition of the deposited layers, thus tailoring the optoelectronic properties of semiconductor compounds. Specifically, the possibility to tune the band gap by varying either the number of deposition cycles or the growth sequence of ternary compounds paves the way toward the formation of advanced photovoltaic materials.

Keywords: E-ALD, Ag(111), thin films, metal chalcogenides, UPD, photovoltaics

1. Introduction

Improving the efficiency of the deposition techniques of compound semiconductors could be crucial for the future sustainable micro and nano-electronic industry. A common challenge

INTECH
open science | open minds

© 2018 The Author(s). Licensee InTech. This chapter is distributed under the terms of the Creative Commons Attribution License (http://creativecommons.org/licenses/by/3.0), which permits unrestricted use, distribution, and reproduction in any medium, provided the original work is properly cited. CC BY

when reviewing current technologies is the lack of reliable compositional control as well as conformal coating of complex geometries. Electrochemical deposition techniques are a low-cost alternative to vacuum evaporation and chemical bath deposition for the direct fabrication of thin films from molecular precursors. Among electrodeposition processes, electrochemical atomic layer deposition (E-ALD) has the advantage to fabricate semiconductors one atomic layer at a time, thus requiring very low energy consumption, diluted solutions, and operating at standard environmental conditions. Fine control of the thin film growth is achieved through the surface limited reaction (SLR), usually referred as under potential deposition (UPD), of the ionic precursors with the electrode substrate or a preceding layer. When the thin film growth can be rigorously considered epitaxial, the E-ALD method is referred as electrochemical atomic layer epitaxy (ECALE) [1]. E-ALD is recognized as a very effective method for the electrodeposition of ultra-thin films of semiconducting materials. In recent years, thin films of binary [2–5] and ternary semiconductors [6–9] were successfully obtained on silver electrodes. **Figure 1** illustrates the steps involved in the E-ALD process of a ternary compound. The chosen sequence for the alternate deposition of different elements dictates both the structure and the stoichiometry of the resulting semiconductor compound.

This chapter highlights the current progress in E-ALD of binary and ternary chalcogenides on Ag(111) from an electrochemical perspective.

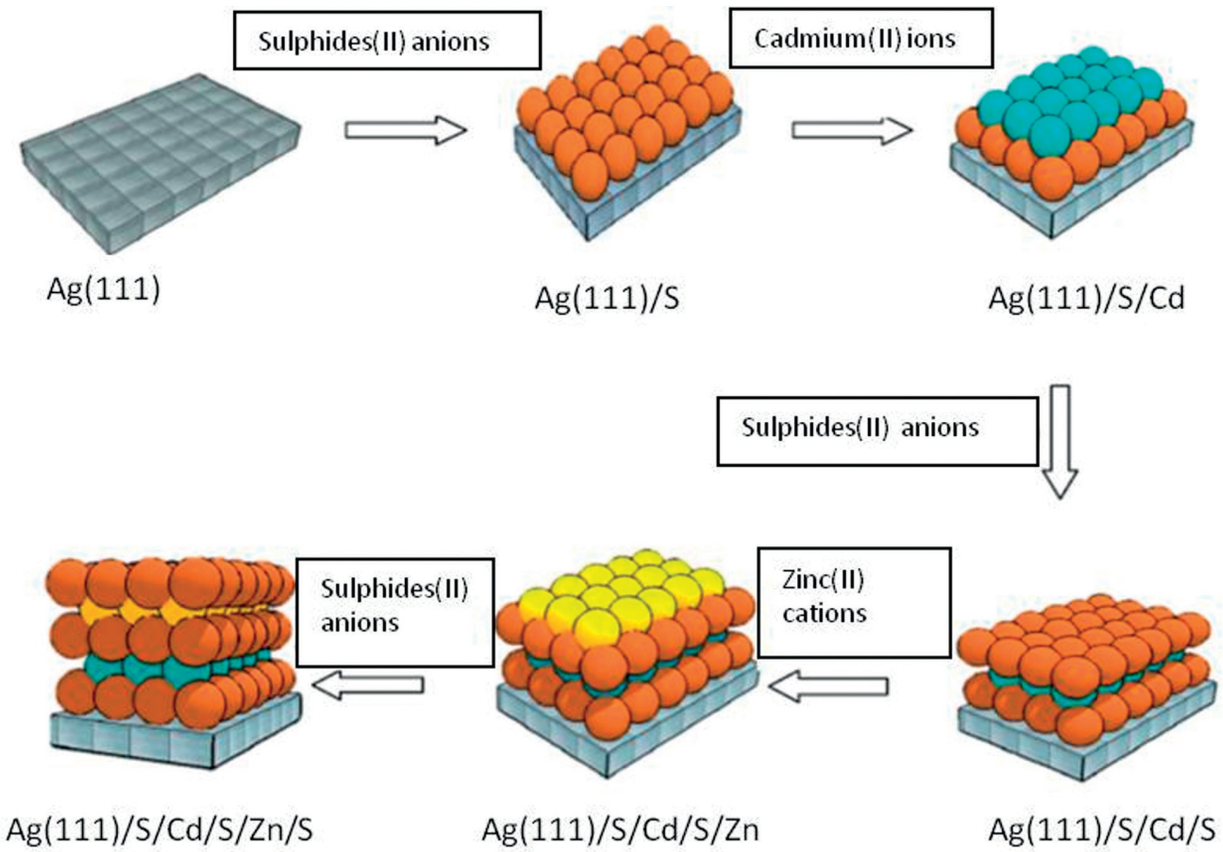

Figure 1. Schematic of the E-ALD growth of a ternary semiconductor. The solutions used in each step are indicated in the boxes below.

http://dx.doi.org/10.5772/intechopen.71014

2. Thermodynamics of the UPD process

For the sake of simplicity and clarity, we will develop the thermodynamics of an epitaxial E-ALD process (ECALE) with the steps constituted by UPD. As a reference we consider the ECALE growth of CdS on Ag(111). From a purely chemical perspective, ECALE exploits UPD to grow the semiconductor compounds on a well-behaving surface. For instance, the oxidative deposition of an atomic layer of sulfur atoms on top of Ag(111) surface is:

$$\mathrm{Ag}(111) - S_{ad} + 2e^- \leftrightarrows \mathrm{Ag}(111) + S^{2-} \tag{1}$$

where S_{ad} refers to the sulfur adlayer. The UPD provides a surface limited deposition process, which is characterized by a potential more cathodic than the bulk deposition. The latter is defined by means of the Nernst equation:

$$E_{S^{2-}/S} = E^0_{S^{2-}/S} + \frac{RT}{2F} ln\left(\frac{a_S}{a_{S^{2-}}}\right) \tag{2}$$

Considering the experimental observation of the potential shift provided by a UPD process, a heuristic extension of the Nernst equation can be proposed:

$$E_{S^{2-}/S_{Ad}} = E^0_{S^{2-}/S} + \frac{RT}{2F} ln\left[\frac{a_{S_{ad}}(\theta)}{a_{S^{2-}}}\right] \tag{3}$$

where $a_{S_{ad}}(\theta)$ is the activity of S atoms adsorbed on Ag(111) as a function of the coverage θ. Rearranging Eqs. (2) and (3) we obtain the underpotential shift, ΔE_{UPD} [10]:

$$\Delta E_{UPD} = E_{S^{2-}/S_{Ad}} - E_{S^{2-}/S} = \frac{RT}{2F} ln\left[\frac{a_{S_{ad}}(\theta)}{a_S}\right] \tag{4}$$

which is, incorrectly, independent from the activity of the sulfide anions. This heuristic approach, though enabling an intuitive description of the UPD process, does not take into account other terms such the local defects of the electrode surface, and the mutual interactions between solvent, surfaces and anions.

A more accurate description of the UPD thermodynamics can be formulated in the framework of the ideal polarized electrode. Following this approach, the substrate (i.e. Ag(111)) on which UPD takes place is in contact with the electrolyte solution (sol) containing S^{2-}, Na^+ and X^- ions and solvent (H_2O). From a theoretical standpoint, the electrolyte solution can be considered in contact with a reference electrode reversible with respect to a general anion X^-. The phases relevant for the present analysis are the Ag(111) surface, the solution (sol), and the interphase (IP) between the substrate and sol. Each phase, j, is described thermodynamically by the Gibbs energy, G^j, which is a function of the variables T^j (temperature), P^j (pressure), A^{IP} (interfacial area) and N_i^j (amount of matter of the i^{th} species):

$$G^j = G^j\left(T^j, P^j, A^{IP}, N_i^j\right) \tag{5}$$

The total derivative of the Gibbs energy gives [10]:

$$dG = \sum_j dG^j = \gamma^{IP} dA^{IP} + \sum_{j,i} S^j dT^j - V^j dP^j + \mu^j dN_i^j \tag{6}$$

where γ^{IP} is the surface tension of the interphase, S^j the entropy, V^j the volume and μ^j the chemical potential.

Let us now consider a solution of Na_2S in NaOH buffer solution (i.e. pH = 13) at constant T^j, P^j. The main charge transfer equilibrium is:

$$S_{sol}^{2-} \leftrightarrows S_{el} \tag{7}$$

where *sol* refers to the liquid phase and *el* refers to the electrode. The corresponding electrocapillary equation is [11, 12]:

$$-d\gamma^{IP} = \Gamma_{S^{2-}}^{IP} d\mu_{S^{2-}}^{sol} + \Gamma_{OH^-}^{IP} d\mu_{OH^-}^{sol} + \Gamma_S^{IP} d\mu_S^{el} - q_{ion} dE \tag{8}$$

where E is the potential referred to the reference electrode and it is defined by means of the chemical potential $\Gamma_{Na^+}^{IP} d\mu_{Na^+}^{sol}$. According to this latter definition, q_{ion} is the surface excess of the electric charge density:

$$q_{ion} = \left(\frac{\partial \gamma^{IP}}{\partial E}\right)_{\left(\mu_{s^{2-}}^{sol}, \mu_{OH^-}^{sol}, \mu_S^{el}\right)} \tag{9}$$

also known as Lippmann equation. $\Gamma_{OH^-}^{IP}$, $\Gamma_{S^{2-}}^{IP}$ and Γ_S^{IP} are the relative excess of Na^+ and S^{2-} with respect to H_2O (solvent):

$$\Gamma_{S^{2-}}^{IP} = \frac{1}{A^{IP}} \left[N_{S^{2-}}^{IP} - \frac{N_{S^{2-}}^{sol} N_{H_2O}^{IP}}{N_{H_2O}^{sol}} \right] \tag{10}$$

It is important to notice that Eq. (10), in the Gibbs theoretical framework, is not a mere change of variable. In fact, the amounts of matter (N_i^{IP}) depend on the arbitrary definition of the interface while the relative excess of matter (Γ_i^{IP}) is independent of the area and the thickness of the interface. Moreover, the contribution of the formation of the S adlayer is described by the term $d\gamma^{IP}$. In this context, using the following well-known equation for the chemical potential in the case of complete dissociation:

$$\mu_{S^{2-}}^{sol} = \mu_{S^{2-}}^{0,sol} + RT \ln a_{S^{2-}} \tag{11}$$

$$\mu_{OH^-}^{sol} = \mu_{OH^-}^{0,sol} + RT \ln a_{OH^-} \tag{12}$$

$$\mu_S^{el} = \mu_S^{el} + RT \ln \theta_S \tag{13}$$

where a is the activity in the liquid phase and θ is the fractional amount in the solid phase. In this framework the relationship between activities and surface tension is well represented by the following:

http://dx.doi.org/10.5772/intechopen.71014

$$\Gamma_{S^{2-}}^{IP} = \frac{1}{RT}\left(\frac{\partial\gamma^{IP}}{\partial \ln a_{S^{2-}}}\right)_{\left(a_{OH^-}^{sol},\theta_S^{el},q_{ion}\right)} \tag{14}$$

$$\Gamma_{OH^-}^{IP} = \frac{1}{RT}\left(\frac{\partial\gamma^{IP}}{\partial \ln a_{OH^-}}\right)_{\left(a_{S^{2-}}^{sol},\theta_S^{el},q_{ion}\right)} \tag{15}$$

$$\Gamma_S^{IP} = \frac{1}{RT}\left(\frac{\partial\gamma^{IP}}{\partial \ln \theta_S}\right)_{\left(a_{S^{2-}}^{sol},a_{OH^-}^{sol},q_{ion}\right)} \tag{16}$$

$$E = \left(\frac{\partial\gamma^{IP}}{\partial q_{ion}}\right)_{\left(a_{S^{2-}}^{sol},a_{OH^-}^{sol},\theta_S^{el}\right)} \tag{17}$$

Hence, the surface tension depends on the activity of the chemical species:

$$\gamma = \gamma_{\left(a_{S^{2-}}^{sol},a_{OH^-}^{sol},\theta_S^{el},q_{ion}\right)} \tag{18}$$

Therefore, upon the integration of Eq. (8), an extension of the Nernst equation can be obtained substituting Eqs. (11)–(13) and (18):

$$E = E^0 + \frac{\Gamma_{S^{2-}}^{IP} RT}{q_{ion}} \ln a_{S^{2-}} + \frac{\Gamma_{OH^-}^{IP} RT}{q_{ion}} \ln a_{OH^-} + \frac{\Gamma_S^{IP} RT}{q_{ion}} \ln \theta_S + \frac{1}{q_{ion}}\left[\gamma_{\left(a_{S^{2-}}^{sol},a_{OH^-}^{sol},\theta_S^{el},q_{ion}\right)} - \gamma^0\right] \tag{19}$$

where

- E^0 is the standard potential of the electrode with respect to the reference electrode,
- $\frac{\Gamma_{S^{2-}}^{IP} RT}{q_{ion}} \ln a_{S^{2-}}$ takes into account the effect of the activity,
- $\frac{\Gamma_{OH^-}^{IP} RT}{q_{ion}} \ln a_{OH^-}$ takes into account the effect of the pH, constant in a buffer solution,
- $\frac{\Gamma_S^{IP} RT}{q_{ion}} \ln \theta_S$ takes into account the effect of the surface coverage: $\theta_S = 1$ for bulk phases, θ_S the fractional amount for compounds and the coverage of adlayers,
- $\frac{1}{q_{ion}}\left[\gamma\left(a_{S^{2-}}^{sol}, a_{OH^-}^{sol}, \theta_S^{el}, q_{ion}\right) - \gamma^0\right]$ takes into account the interaction with Ag(111),

Eventually, we should state that Eq. (19), in principle, takes into account all the effects neglected by Eq. (3), thus describing the equilibrium of a system defined by three components, as predicted by the phase rule. Experimental observations suggest that the potential of the UPD process of sulfur depend on the concentration of sulfur atoms ($a_{S^{2-}}$), the pH (a_{OH^-}) and the coverage of the adlayer (θ_S).

3. E-ALD of metal chalcogenides

E-ALD of metal chalcogenides involves sequential SLR of metal and chalcogenides ions. Except for few cases, the choice of chalcogenides as first layer is preferred for its higher affinity for silver and to avoid alloy formation with the electrode substrate [2]. In the E-ALD methodology a monolayer of the compound is obtained by alternating underpotential deposition of the metallic element with the underpotential deposition of the non-metallic element in a cycle, so the thickness of deposited film is a function of the numbers of deposition cycles. **Figure 2a** shows the cyclic voltammogramm of 0.5 mM Na_2SeO_3 on Ag(111) and of $ZnSO_4$ on Se-covered Ag(111). The cathode peak C_{Se} at −0.95 V corresponds to the bulk reduction of the Se. At more negative potentials hydrogen evolution prevents the detection of the Se_{ad} reduction. Zn adlayers deposited on a Se-covered Ag(111) show a CV profile shifted to more positive potential with a reduction peak C_{Zn} at −0.65 V. To prevent Se dissolution, the operating potential for the surface limited deposition of Zn on Ag/Se should be more positive than C_{Se}. Anodic stripping analysis as a function of the applied potential allow to choosing the optimal conditions for the UPD process, which in this case is in the range $-0.95 < E < -0.8$ V, where a plateau at $Q = 60$ μC cm^{-2} is observed (see **Figure 2b**). Alternate depositions of both chalcogenide and metal can be repeated as many times as necessary to form a compound with the desired thickness and composition. **Figure 2c** shows the charges involved in the layer-by-layer growth of Zn and Se in a 1:1 ratio.

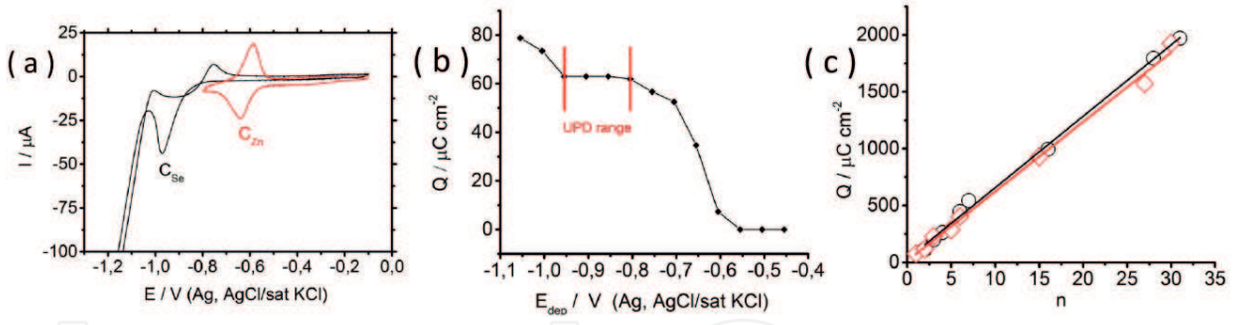

Figure 2. (a) Cyclic voltammograms of (—) Se on Ag(111) and (—) Zn on Se-covered Ag(111) in ammonia buffer solutions (pH 9.2); (b) charges involved in the stripping of Zn, underpotentially deposited on Ag(111)/Se_{ad}, as a function of the deposition potential; (c) charges involved in the striping of (○) Se and (□) Zn as a function of the number of E-ALD cycles. The solid lines represent the linear fit to the data.

4. Flow cell apparatus and experimental conditions

E-ALD thin films of metal chalcogenides were grown on silver single crystal disks using an automated deposition apparatus consisting of Pyrex solution reservoirs, solenoid valves, a distribution valve and a flow-cell [2]. The solutions contained in the Pyrex reservoirs are previously degassed and then constantly kept under a nitrogen pressure $p(N_2) = 0.3$ atm. **Figure 3a** shows the distribution valve with seven solution inlets, in the top, and one solution

http://dx.doi.org/10.5772/intechopen.71014

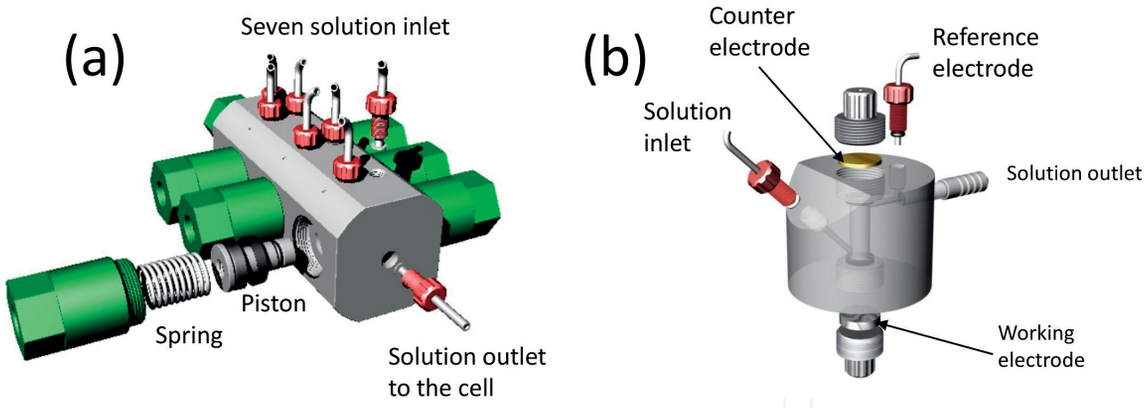

Figure 3. (a) Distribution valve and (b) electrochemical cell.

outlet, in the front. The solution is pushed to the distribution valve by the N_2 overpressure. The inlet of the solution is blocked by a piston of the distribution valve, which is tightly held in place by a spring. The piston can be raised by opening the solenoid valve and sending compressed air at 6 atm, which is higher than the pressure exerted by the spring. The piston is raised enough to allow the solution to flow into the cell. Different solutions are pushed to the cell following the desired sequence by acting on the corresponding solenoid valves. The nitrogen pressure exerted on the solutions determines a flow rate of about 1 mL s^{-1}. All operations are carried out under computer control.

The electrochemical cell (**Figure 3b**) is a Teflon cylinder with a height of 40 mm, an internal diameter of 10 mm and external diameter of 50 mm. The working electrode at the bottom of the cylinder and the counter electrode on top delimit the electrochemical cell volume (1.6 mL). The solution inlet and outlet are placed on the side walls of the cylinder; for hydrodynamic reasons, the inlet is inclined. The working electrode was silver disks cut according to the Bridgman technique [13]. The counter electrode was a gold foil, and the reference electrode was an Ag/AgCl (saturated KCl) placed in the outlet tubing. Leakage is avoided by pressing both the working and the counter electrode against a suitable Viton® O-ring. All potentials reported in the paper are quoted with respect to the Ag/AgCl (saturated KCl) reference electrode.

5. E-ALD of binary M_xS_y semiconductors on Ag(111)

E-ALD technique has been successfully used to fabricate ultrathin films of metal sulfides on silver electrodes by alternating the underpotential deposition of metal and sulfur. These compounds include cadmium sulfide (CdS) [2, 14, 15], zinc sulfide (ZnS) [2], nickel sulfide (NiS) [4], lead sulfide (PbS) [16], copper sulfides (Cu_xS) [17, 18] and tin sulfides (Sn_xS_y) [19]. A typical E-ALD cycle includes the underpotential deposition of sulfur followed by the surface limited reaction (SLR) of metal on S-covered Ag. The UPD of sulfur on crystalline and polycrystalline silver have been extensively investigated in the past [20–22]. Electrochemical measurements on Ag(110), Ag(100) and Ag(111) show that sulfur UPD deposition processes differ significantly on

the three silver facets and in situ STM experiments have evidenced the presence of differently ordered sulfur structures depending on substrate orientation. The formation of the first layer of S on Ag(100) and Ag(110) occurs at a potential of $E = -0.8$ V in pH 13 solutions, whereas on Ag (111) it was obtained at $E = -0.68$ V in ammonia buffer (pH 9.6). Proceeding toward more positive potentials in the presence of sulfide ions resulted in bulk sulfur deposition. Cyclic voltammogramms performed in Na_2S solutions revealed two distinct behaviors. While on Ag (100) only two broad anodic peaks at −1.32 and −1.15 V were observed, cycling the potential on the other two faces resulted in a more complex behavior, with a sharp anodic peak occurring at $E = -1.06$ and $E = -0.78$ on Ag(110) and Ag(111), respectively. The charges associated with the UPD deposition of S in the first layer, as calculated from chronocoulometry experiments, were 137μC cm^{-2} for Ag(100), 163μC cm^{-2} for Ag(110) and 189μC cm^{-2} for Ag(111). Although the growth of M_xS_y on silver electrodes follows an oxidative-reductive behavior in all cases, SLR of metal layers depends on the semiconductor type and solution conditions.

5.1. E-ALD of PbS and NiS

Lead sulfide (PbS) and nickel sulfide (NiS) are binary semiconductors that have received considerable attention for a variety of applications, such as detectors [23], sensing materials [24] and solar cells [25]. A complete electrochemical study of PbS multilayers has been reported by Fernandes et al. [16]. The Pb_{ad} cannot be formed on S-covered silver electrodes because of partial redissolution of sulfur. So the first layer is the Pb_{UPD} deposited on Ag(111), this was obtained from 5.0 mM $Pb(NO_3)_2$ solutions in acetic buffer at pH 5 by scanning the potential from −0.2 to −0.45 V. Two well-defined peaks were observed at −0.35 and −0.29 V for the deposition and the dissolution of Pb monolayer, respectively. Next, the underpotential deposition of S on Pb-covered Ag(111) was obtained by scanning the potential from −1.0 to −0.70 V in 2.5 mM Na_2S solutions in ammonia buffer. The constancy of the anodic stripping of Pb deposited at −0.45 V and at different accumulation times ensures the process is surface limited, giving rise to a charge of 332 μC cm^{-2} for the first layer. Successive sulfur and lead layers resulted in a linear growth with an average charge per cycle of approximately 83 μC cm^{-2}. Morphological analysis by ex-situ AFM measurements revealed the deposits consisted of homogeneous films of PbS small clusters.

Differently from lead, underpotential deposition of nickel on bare Ag(111) is not possible due to weak adhesion with the electrode substrate and competing surface phase transformations [26]. On the contrary nickel presents a well-defined surface limited reaction on S-covered Ag (111), showing cathodic and anodic peaks at −0.52 and −0.22 V, respectively. UPD layers of nickel were obtained from $NiCl_2$ in boric acid solutions (pH 6.5) at $E = -0.6$ V. The amount of sulfur, as determined by separate anodic stripping experiments, was found to increase linearly with the number of the deposition cycles. Conversely, the stripping of nickel was less precise due to the formation of oxide and hydroxide films with the increase in layer number [27]. Despite these limitations the charges of both Ni and S showed a quasi-linear layer-by-layer growth with slopes of 53 μC cm^{-2} for Ni and 58 μC cm^{-2} for S. Morphological analysis by AFM indicated a decrease of average roughness with aging, thus suggesting the formation of a passivation layer with time, which was later confirmed by XPS analysis.

5.2. E-ALD of CdS, ZnS, Sn_xS_y and Cu_xS

Cadmium, tin, zinc, and copper are metals that form strong interactions with sulfur ions, thus generating binary semiconductors with peculiar transport and electrical properties. Cadmium and zinc sulfides have been among the first binary semiconductors to be deposited by means of E-ALD due to favorable electrochemical characteristics.

UPD deposition of CdS has been investigated on silver single crystals exhibiting different orientations, that is, Ag(111), Ag(110) and Ag(111) [14, 15].The well-defined structures of S_{UPD} formed on silver electrodes in Na_2S ammonia buffer solutions drive the epitaxial deposition of the subsequent Cd layer. After washing out the sulfur ions in excess, UPD of cadmium is performed by holding the potential at −0.68 V on S-Ag(111) and at E = −0.6 V on the other two faces. The procedure used to obtain further alternate S and Cd layers is identical with that used for the Ag/S/Cd structure. The average values of the charge deposited in each E-ALD cycle were 103 μC cm^{-2} for Ag(100), 85 μC cm^{-2} for Ag(110) and 70 μC cm^{-2} for Ag(111). Ex situ XPS analysis confirmed the presence of cadmium and sulfur in a 1:1 stoichiometric ratio [28, 29].

Similarly to cadmium sulfide, E-ALD of ZnS thin film were grown on silver electrodes by first depositing sulfur at E = −0.70 V from Na_2S solution, and then injecting $ZnSO_4$ solution while keeping the electrode at the same potential to deposit Zn underpotentially. Plots of the charges for Zn and S measured in the stripping of ZnS deposits were linear, with a slope of 67 μC cm^{-2} for Zn and 75 μC cm^{-2} for S [2].

Differently from CdS and ZnS, the other two metal sulfides (Cu_xS and Sn_xS_y) exist in different stoichiometric ratios and morphologies; their interest in E-ALD growth relies on the tunable transport and electronic properties by changes in composition, x and y [30, 31].

The surface limited reaction of Sn_xS_y has been thoroughly studied by Innocenti et al. [19] both on bare and on S-covered silver substrates. Electrodeposition of tin on bare silver showed two anodic peaks, E_{c1} = −0.70 V and E_{c2} = −0.48 V, the latter ascribed to the formation of Sn(IV) hydroxides. Differently, on S-covered Ag(111) the reduction peak was seen at lower potentials, E_c = −0.61 V, thus suggesting true underpotential deposition mechanism. Independently from the deposition time, the charge involved in the oxidative process remained nearly constant, thus confirming a surface limited process.

Thin films of copper sulfides were fabricated on silver substrates through E-ALD. Although surface limited the layer-by-layer growth of Cu_xS was found not to be a true UPD process like for the other metal sulfides. As reported by Innocenti et al. [17] the electrochemistry of copper on S-covered Ag(111) is quite complex. Cyclic voltammograms as obtained by sweeping the potential between −0.05 and −0.55 V in 1 mM Cu(II) solutions in ammonia buffer revealed the presence of two cathodic peaks, E_1 = −0.39 V and E_2 = −0.42 V. While the latter was easily associated to the bulk reduction of Cu(II) to Cu(0), the nature of the first cathodic peak is still under debate, except for the fact that it precedes bulk deposition. More-in-depth electrochemical analysis suggests the process is surface limited in the range −0.3 to −0.38 V and it involves the formation of Cu(0) through the two-step reduction of cupric tetra-amino complex and the subsequent conproportionation reaction:

$$Cu(NH_3)_4^{2+} + e^- \rightarrow Cu(NH_3)_2^+ + 2NH_3 \quad (20)$$

$$Cu(NH_3)_2^+ + e^- \rightarrow Cu(0) + 2NH_3 \quad (21)$$

$$Cu(NH_3)_4^{2+} + Cu(0) \rightarrow 2Cu(NH_3)_2^+ \quad (22)$$

The amount of Cu deposited in a given number of cycles was determined by measuring the charge involved in the anodic stripping. The authors found the charges were linearly increasing with the number of deposition cycles with a slope of 44 μC cm^{-2}. XPS results confirmed the valence states of copper and sulfur as Cu(I) and S(−II), respectively, although a possible fraction of S(−I) in the form of disulfide anion was not excluded. The experimental Cu/S ratio observed in the XPS characterization was later attributed to the covellite phase, where positive holes allow Cu ions to be stabilized in their monovalent state [32]. The morphological analysis by AFM was able to evidence the low roughness values of the deposits, thus confirming the high homogeneity and good quality of the thin film obtained.

5.3. E-ALD of ternary $M_xN_{1-x}S$

The interest in cadmium, zinc, tin, and copper sulfides has increased in the last 10 years due to the possibility to fabricate ternary semiconductor compounds, thus allowing fine control over the band gap energy of solar cell devices [32–34]. E-ALD method has been successfully employed to grow ternary materials such as $Cd_xZn_{1-x}S$ [35, 36], $Cu_xZn_{1-x}S$ [5] and $Cu_xSn_yS_z$ [33]. These semiconductors were prepared by sequential deposition of the corresponding binaries; for instance, alternate deposition of Cu_xS and Sn_xS_y was carried out to form $Cu_xSn_yS_z$. Because of the large variety of the possible (x:y:z) combinations research on E-ALD of multinary kesterite group thin films, although challenging, is quite promising for the development of non-linear electro-optic devices and photovoltaic cells. Depending on the adopted sequence profile only certain combinations were attainable, thus limiting the possible metal-to-metal stoichiometries. The electrochemical behavior of $Cu_xSn_yS_z$, $Cu_xZn_{1-x}S$ and $Cd_xZn_{1-x}S$ thin films is separately discussed below.

Di Benedetto et al. [33] investigated the electrodeposition of $Cu_xSn_yS_z$ thin films exploiting different sequences of E-ALD cycles, that is $Ag/S[(Cu/S)_k/(Sn/S)_j]_n$ with k = 1, j = 1, 2 and $1 < n < 60$. Surface limited deposition of Cu and Sn occurred, respectively, at $E = -0.37$ V and $E = -0.68$ V in ammonia buffer containing EDTA. As already reported for binary sulfides S_{UPD} layers on Ag(111) and on metal were obtained by keeping the potential at $E = -0.68$ V in Na_2S ammonia solutions. Stripping analysis of the ternary sulfides yielded a large and well-defined peak centered at $E = -0.22$ V (Cu stripping), preceded by a broader peak at −0.43 V (Sn stripping). Charges involved in the stripping of both metals (Sn + Cu) and S allowed defining the effective layer-by-layer formation of a ternary compound with a slope of 42 μC cm^{-2}, which is very close to the value obtained from the stripping of the binary CuS compound [19]. The chemical composition of $Ag/S[(Cu/S)_k/(Sn/S)_j]_n$ deposits were analyzed by means of SEM, XPS and TOF-SIMS [37]; the ex-situ characterizations have highlighted the nominal stoichiometry is not respected leading to Sn/Cu ratio equal to 1/13 and 1/9 for j = 1, and 2, respectively. Independently from Sn/Cu ratio the morphology of the growing films, as revealed

by AFM measurements, were found to be homogeneous and similar to the bare Ag(111). Conversely, the band gap values, carried out by diffuse reflectance spectroscopy, decreased with the increase in thickness and Cu/Sn ratio ranging from 2.12 for $n = 60$, $j = 2$–2.43 eV for $n = 20$, $j = 1$.

As for the Cu-Sn-S system the experimental conditions to grow ternary cadmium and zinc sulfides on Ag(111) with the E-ALD were by alternating the underpotential deposition of the corresponding binaries (CdS and ZnS) [36]. The potential chosen for the deposition of S and Zn was −0.65 V, whereas different series of experiments were carried out depositing Cd in correspondence to the first (−0.5 V) or to the second UPD (−0.65 V). The authors investigated the electrodeposition of $Cd_xZn_{1-x}S$ thin films exploiting different sequences of E-ALD cycles, that is, $Ag/S[(Cd/S)_k/(Zn/S)_j]_n$ with $k = 1$, $j = 1$, 2, 5 and $1 < n < 20$. The charge involved in the stripping increases linearly with the number of deposition cycles. Yet, the slope of the plot decreases while increasing the number of ZnS cycles per CdS cycles, that is, 89, 67 and 52 μC cm^{-2} for $j = 1$, 2 and 5, which reflect the higher percentage of Zn in the deposit. The chemical composition of $Cd_xZn_{1-x}S$ thin films, as analyzed by XPS have highlighted the nominal stoichiometry is not respected leading to Zn/Cu ratio equal to 1/3, 1/2 and 2 for $j = 1$, 2 and 5, respectively. However, regardless of the stoichiometry of the obtained ternary compound, the charge involved in cathodic stripping was equal to the charge involved in the anodic one, thus indicating the right 1:1 stoichiometric ratio [35].

The low contribution of Zn in $Cd_xZn_{1-x}S$ compounds was also found to occur in the Cu-Zn-S system. Ternary Cu_xZn_yS compounds were obtained through the E-ALD method by alternating deposition of Cu_xS and ZnS layers. Innocenti et al. [8, 38] studied the electrochemical and compositional behavior of $Cd_xZn_{1-x}S$ thin films by applying the general sequence $Ag/S/[(Cu/S)_j/(Zn/S)_k)]_n$ with $j = 1$, $k = 1$, 5, 9, and $1 < n < 60$. As for other binary and ternary compounds UPD sulfur layers were obtained by keeping the electrode potential at E = −0.68 V for either on bare Ag(111) or on Ag(111) already covered by a metal layer. Deposition of Cu and Zn occurred in ammonia buffer at −0.37 and −0.85 V, respectively. Stripping analysis revealed the charge involved in (Cu + Zn) deposition followed a nonlinear increase with the number of cycles. Moreover, samples containing higher percentage of Zn had lower slope, thus indicating a lower extent of deposition in each cycle; a Cu/Zn ratio of about 6 was found for $j = 1$, $k = 1$, and $n = 40$. From the plot of charges against the number of deposition cycles (n) we expect a ZnS:CuS equimolar ratio for n = 13. Zn deficiency upon increasing the cycles is due to partial redissolution of zinc during the E-ALD of copper, thus causing a rearrangement in the adlayers. Independently from the Cu/Zn ratio, ex-situ investigations highlighted at least two prevailing morphologies, the first one homogeneously covering the Ag(111) surface, and the second one consisting of random network of nanowires of variable length [8].

6. E-ALD of binary M_xSe_y semiconductors on Ag(111)

The E-ALD of metal selenides (M_xSe_y) on monocrystalline surfaces usually starts with the deposition of a selenium monolayer by using selenite, Se(IV), as a precursor salt. Differently

from sulfur deposition the oxidative UPD of Se is not allowed due to the low stability of selenite solutions. According to the work by Rajeshwar et al. [39] the electrochemistry of Se (IV) is quite complex. The direct reduction of Se(IV) to Se(0) is attributed to the formation of the electroinactive gray Se, which forms a stable deposit:

$$H_2SeO_3 + 4H^+ + 4e^- \rightarrow Se + 3\,H_2O \tag{23}$$

Instead, the electroactive form of Se(0), usually referred as red Se, is obtained through a first reduction of Se(IV) to Se(−II) followed by a comproportionation reaction [40]:

$$H_2SeO_3 + 6H^+ + 6e^- \rightarrow H_2Se + 3\,H_2O \tag{24}$$

$$H_2SeO_3 + H_2Se \rightarrow 3Se + 3\,H_2O \tag{25}$$

In ammonia buffer (pH 9.3), the presence of the electroactive red Se is evident for $E < -0.95$ V through the reduction Se(0) → Se(−II), and around $E = -0.8$ V through the oxidation Se (0) → Se(IV). Adlayers of Se on the electrode surface, Se_{ad}, are formed through a two-step procedure involving the deposition of an excess of Se(0) from Se(IV) solutions, followed by the reduction of bulk Se at sufficiently negative potential ($E \approx -0.95$ V). The reduction must be performed in the absence of Se(IV) to avoid the comproportionation reaction with Se(−II) leading to a massive formation of Se(0). The STM investigation at potential more negative than the bulk reduction peak has shown two distinct structures. The layer at more positive potentials has a ($\sqrt{7} \times \sqrt{7}$) R19.1° structure, with an associated charge of 65 μC cm^{-2}, whereas at more negative potentials it has a ($2\sqrt{7} \times 2\sqrt{7}$) R19.1° structure, with an associated charge of 48 μC cm^{-2} [41].

6.1. E-ALD of CdSe and ZnSe

Cadmiun selenide is a promising material for application as thin film solar cells [42, 43], quantum dots [44, 45] and p-n junctions [46, 47]. ZnSe is an ideal candidate for optoelectronic devices, especially blue laser and blue emitters.

The E-ALD methodology has been successfully used for the growth of CdSe and ZnSe on Ag (111) [48, 49]. For the growth of CdSe, Se_{ad} was deposited from a 0.5 mM Se(IV) in a pH 8.5 ammonia buffer solution for 30s at a fixed potential $E = -0.9$ V; then the solution was replaced with the supporting electrolyte alone, and a potential $E = -0.9$ V was applied for 60s to reduce the bulk Se(0). The reductive underpotential deposition of Cd from a 1 mM $CdSO_4$ in a pH 8.5 ammonia buffer solution on a Se-covered Ag(111) substrate, has 2 peaks. A well-defined UPD peak is observed at $E = -0.41$ V, whereas the beginning of a second UPD peak is observed at $E = -0.69$ V. The second UPD peak cannot be completely recorded, since it overlaps bulk Cd deposition and it can never be isolated from bulk Cd deposition. The optimal conditions for the adlayer formation of Cd on Se-covered Ag(111) are by keeping the electrode at $E = -0.55$ V for 30 s. The plots of the charges for Cd and Se stripping as a function of the number of ECALE cycles are linear, with an average charge per cycle of approximately 75 μC cm^{-2}. The coincidence of the charges associated with each layer of Cd and Se gives a 1:1 stoichiometric ratio between the elements as expected for CdSe.

For the growth of ZnSe, Se_{ad} was deposited from a 0.5 mM Se(IV) in a pH 9.2 ammonia buffer solution for 60 s at potential −0.95 V; then, the solution was replaced with the supporting electrolyte alone, and a potential $E = -0.95$ V was applied for 60 s to reduce the bulk Se(0). The Zn UPD on a Se-covered Ag(111) is obtained at $E = -0.8$ V for 30 s from 1 mM $ZnSO_4$ in a pH 9.2 ammonia buffer solution. Once the deposit was formed, the amount of elements deposited in a given number of cycles was estimated from the charge involved in their stripping. The plots of the charges for Zn and Se stripping as a function of the number of cycles are linear, with a charge per cycle of 61 μC cm^{-2} for Zn and 63 μC cm^{-2} for Se.

6.2. E-ALD of $Cd_xZn_{1-x}Se$

The electrochemical conditions necessary to form CdZnSe deposits by E-ALD on Ag(111) are described in the works by Loglio et al. [36, 50]. The first atomic layer on Ag(111) is obtained by SLR of selenium, as previously described. The UPD deposition on Se-covered Ag(111) from ammonia buffer of Cd would cause Zn redissolution. To shift Cd_{UPD} toward more negative potentials it is necessary to use a stronger complexing agent, that is, 0.1 M pyrophosphate in 0.01 M NaOH, and slightly shifting the Zn UPD toward more positive potentials using acetic buffer at pH 5.0. The experimental procedure to obtain $Cd_xZn_{1-x}Se$ with different x values consists of alternating ZnSe and CdSe ECALE cycles with different deposition sequences. The reductive UPD of Cd on a Se-covered Ag(111) substrate, from a 1 mM Cd(II) solution, was obtained by applying a potential $E = -0.7$ V for 60 s. In an analogous way, ZnSe was obtained by depositing Zn, from a 1 mM Zn(II) solutions, at $E = -0.8$ V. The stripping analysis of the compound obtained with 100 deposition (CdSe + ZnSe) cycles revealed a very high percentage of Cd (74%).

The most effective way to increase the amount of Zn in the deposit consists of depositing more ZnSe cycles per CdSe cycle. The x stoichiometric parameter is a linear function of the ZnSe/CdSe sequence; $x = 0.5$ was obtained with the ZnSe/CdSe sequence equal to 5.

The charge involved in stripping the cations equals the charge involved in stripping the anions, thus confirming the right 1:1 stoichiometric ratio calculated from XPS data. The charge per cycle changes while changing the ZnSe/CdSe sequence, a minimum at $x = 0.5$ is observed, with two symmetrical branches around the minimum. When the percentage of Zn in the compound is approximately equal to that of Cd, the different structures (Zincblend and Wurtzite) are present in a comparable amount, thus suggesting a structural disorder that could be responsible for a reduced amount of deposition.

7. E-ALD of M_xTe_y semiconductors on Ag(111)

The E-ALD of metal tellurides, M_xTe_y, on monocrystalline surfaces starts with the deposition of tellurium. As in the case of selenite, telluride solutions are not stable, so the oxidative UPD is

not allowed. Te(IV) reduction occurs following two possible schemes [51, 52]. A stable Te deposit is formed upon direct reduction of Te(IV)

$$H_2TeO_2^+ + 3H^+ + 4e^- \rightarrow Te + 2\,H_2O \tag{26}$$

or through a two-step process involving the reduction of Te(IV) to Te(−II) followed by a comproportionation reaction

$$H_2TeO_2^+ + 5H^+ + 6e^- \rightarrow H_2Te + 2\,H_2O \tag{27}$$

$$H_2TeO_2^+ + 2H_2Te \rightarrow 3Te + 2\,H_2O + H^+ \tag{28}$$

The TeO_2 in ammonia buffer solutions (pH 8.5) on Ag(111) shows a large reduction peak at E = −0.4 V, which is only observed during the first scan from −0.1 to −0.9 V. Integration of the peak yields a charge of about 370 μC cm^{-2}. Due to the high irreversibility of the system, the reoxidation of the underpotentially deposited Te is prevented by silver oxidation, so the Te UPD peak disappears in the successive CV scans. At about −1.1 V only bulk Te(0) reduction occurs. Te UPD layer starts the reduction at potentials more negative than −1.5 V because of higher bonding energy with the silver substrate.

So, the Te_{ad} can be obtained through UPD reduction before bulk deposition or in a two-step process: deposition at a potential of −0.6 V of small excess of bulk Te, followed by the reduction of bulk Te (but not Te_{ad}) at a potential of −1.4 V.

7.1. E-ALD of CdTe

CdTe deposition on Ag(111) was obtained by E-ALD method [53], alternating UPD of tellurium and cadmium. The formation of the first layer of Te on Ag(111) is obtained by a two-step procedure instead of the direct deposition before the bulk reduction, previously described. This choice allows to having the same standard sequence for all cycles, which can be repeated as many times as desired.

The second step of the ECALE cycle is the underpotential deposition of the metallic element on the silver substrate covered by the non-metallic element. UPD of cadmium on Te-covered electrode occurs from 0.5 mM Cd(II) in ammonia buffer solution at a potential of −0.6 V, more negative than on bare Ag(111). Cadmium cyclic voltammograms, obtained from 0.5 mM Cd(II) in an ammonia buffer solution, do not exhibit narrow and sharp peaks as in the case of Te_{ad}. This finding could be attributed to a partial overlap with a second UPD peak, which in turn cannot be easily isolated from the concomitant beginning of bulk deposition. The second Te_{ad} layer cannot be obtained by the direct deposition before the bulk reduction, since underpotential deposition of Te occurs at a more positive potential than Cd stripping. Therefore, the two-step procedure described above has been adopted. The plots of the charges for Cd and Te stripping as a function of the number of cycles are linear, with an average charge per cycle equal to about 175 μC cm^{-2} for Cd and 155 μC cm^{-2} for Te. The ratio Cd/Te determined on the basis of electrochemical measurements is very close to the 1:1 stoichiometric ratio, which is indicative of a compound formation. The linear behavior suggests a layer-by-layer growth.

8. E-ALD of CdS_xSe_{1-x} on Ag(111)

Cadmium chalcogenides such as CdSe and CdS are excellent materials for the development of high efficient and low-cost photovoltaic devices. The small lattice mismatch between CdS and CdSe allows the formation of cadmium sulfoselenides CdS_xSe_{1-x} over a wide range of compositions ($0 < x < 1$), thus covering the visible solar spectrum from $E = 2.44$ eV for $x = 1$ to $E = 1.72$ eV for $x = 0$ [54, 55].

The first ECALE study on ternary CdS_xSe_{1-x} compounds has been reported by Foresti et al. on Ag(111) substrates by alternating the underpotential deposition of CdSe and CdS layers [56]. To obtain CdSe, cadmium was deposited on Se-covered silver substrates from 1 mM Cd(II) solution in ammonia buffer (pH 9.6) by applying a potential $E = -0.5$ V for 60s. The formation of the first layer of Se on Ag(111) were obtained by a two-step procedure as described before [36]. After Cd deposition the cell was rinsed with ammonia buffer and the ECALE cycle was then completed by depositing CdS. The S_{UPD} layer was obtained by applying a potential $E = -0.68$ V for 60s followed by washing with ammonia buffer. Finally, the reductive underpotential deposition of cadmium was attained on a S layer from 1 mM Cd(II) solutions by keeping the electrode at $E = -0.65$ V. The alternated deposition of CdSe and CdS can be repeated as many times as desired to obtained deposits of variable thickness and composition. The authors investigated different sequences of E-ALD cycles, that is $Ag/[(Cd/Se)_j/(Cd/S)_k)]_n$ with $j:k = 1:1$, $j:k = 2:3$ and $1 < n < 100$. Independent from the sequence, CdSe deposition appeared to be favored with respect to CdS growth leading to the formation of sulfoselenides with $x = 0.2$ and 0.4 for $j:k = 1:1$ and 2:3, respectively. The charges involved in the stripping increase linearly with the number of deposition cycles, thus supporting a layer-by-layer growth. Regardless of the stoichiometry of the ternary compound obtained, the two charges are equal, thus confirming the right 1:1 stoichiometric ratio between Cd and (S + Se). Ex situ AFM measurements as a function of composition indicated the roughness decreased while increasing the S percentage, which determines a better deposit. Photoelectrochemical measurements on CdS_xSe_{1-x} ternary compounds revealed a monotonic band gap dependence with x, thus confirming the formation of a single homogeneous phase.

9. Conclusions

The E-ALD is a very inexpensive method for the production of high-crystalline thin film semiconductors. Exploiting Surface Limited Reactions (SLRs) on electrode surfaces allows the layer-by-layer deposition of different atomic elements. The E-ALD has been successfully used to grow ultra-thin films of metal chalcogenides on silver single crystals. The electrochemistry of binary compounds indicates that, with only the exception of the first layer, the charge associated with each layer of either metal or chalcogenide has the same average value. The layer in direct contact with the silver substrate can be regarded as an interface between the metal and the semiconductor electrodeposited on it. Semiconductors grown on Ag(111) by means of E-ALD are characterized by a high crystallinity of the materials and good photoconversion efficiencies. The ability to control the thickness of the deposited layers allows

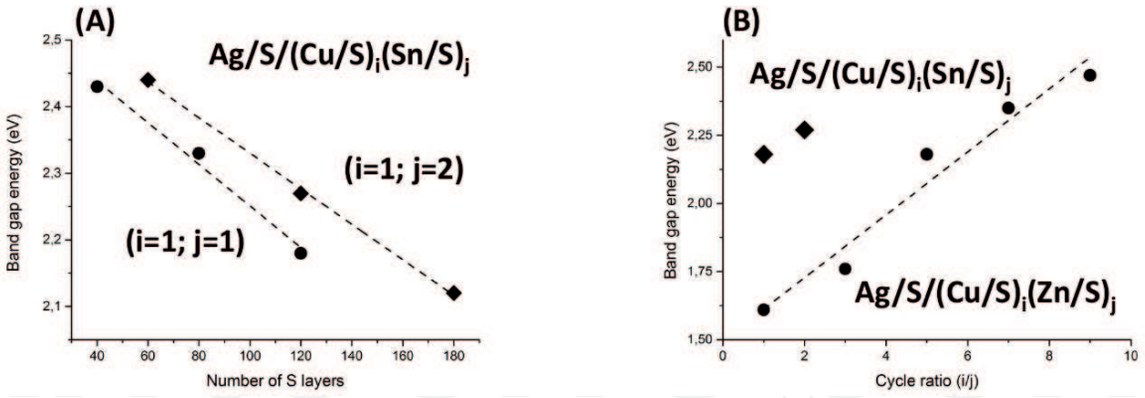

Figure 4. Experimental band gap values (markers) of ternary compounds as a function of (A) thickness at fixed composition and (B) Cu ratio at fixed number of S layers, n = 121. The dotted lines are the linear fit to the data.

fine tuning the semiconductor transition energy by varying the number of deposition cycles (**Figure 4A**). Moreover, careful design of the growth sequence of ternary compounds direct the formation of advanced photovoltaic materials having compositionally controlled band gaps (**Figure 4B**).

Author details

Emanuele Salvietti[1], Andrea Giaccherini[1], Filippo Gambinossi[1], Maria Luisa Foresti[1], Maurizio Passaponti[1], Francesco Di Benedetto[2] and Massimo Innocenti[1]*

*Address all correspondence to: m.innocenti@unifi.it

1 Department of Chemistry, University of Florence, Sesto Fiorentino, Italy

2 Department of Earth Sciences, University of Florence, Florence, Italy

References

[1] Gregory BW, Stickney JL. Electrochemical atomic layer epitaxy (ECALE). Journal of Electroanalytical Chemistry. 1991;**300**:543-561

[2] Innocenti M, Pezzatini G, Forni F, Foresti ML. CdS and ZnS deposition on Ag (111) by electrochemical atomic layer epitaxy. Journal of the Electrochemical Society. 2001;**148**:C357-C362

[3] Innocenti M, Forni F, Pezzatini G, Raiteri R, Loglio F, Foresti ML. Electrochemical behavior of As on silver single crystals and experimental conditions for InAs growth by ECALE. 2001;**514**:75-82

[4] Loglio F, Innocenti M, Jarek A, Caporali S, Pasquini I, Foresti ML. Nickel sulfur thin films deposited by ECALE: Electrochemical, XPS and AFM characterization. Journal of Electroanalytical Chemistry. 2010;**638**(10):15-20

[5] Innocenti M, Becucci L, Bencistà I, Carretti E, Cinotti S, Dei L, Di Benedetto F, Lavacchi A, Marinelli F, Salvietti E, Vizza F, Foresti ML. Electrochemical growth of Cu-Zn sulfides. Journal of Electroanalytical Chemistry. 2013;**710**:17-21

[6] Loglio F, Innocenti M, Pezzatini G, Foresti ML. Ternary cadmium and zinc sulfides and selenides: Electrodeposition by ECALE and electrochemical characterization. Journal of Electroanalytical Chemistry. 2004;**562**(1):17-125

[7] Innocenti M, Becucci L, Bencistà I, Carretti E, Cinotti S, Dei L, Di Benedetto F, Lavacchi A, Marinelli F, Salvietti E, Vizza F, Foresti ML. Ternary cadmium and zinc sulfides and selenides: Electrodeposition by ECALE and electrochemical characterization. Journal of Electroanalytical Chemistry. 2013;**70**:17-21

[8] Innocenti M, Cinotti S, Bencistà I, Carretti E, Becucci L, Di Benedetto F, Lavacchi A, Foresti ML. Electrochemical growth of Cu-Zn sulfides of various stoichiometries. Journal of the Electrochemical Society. 2014;**161**(1):D14-D17

[9] Di Benedetto F, Cinotti S, Guerri A, De Luca A, Lavacchi A, Montegrossi G, Carlà F, Felici R, Innocenti M. Physical characterization of thin films of $Cu_xZn_yS_z$ for photovoltaic applications. ECS Transactions. 2013;**58**(11):59-65

[10] Oviedo OA, Reinaudi L, Garcia SG, Leiva EPM. Underpotential Deposition. Switzerland: Springer; 2015

[11] Parsons R. Comprehensive Treatise of Electrochemistry. Vol. 1. Switzerland: Springer; 1980

[12] Jain S, Willander M, Van Overstraeten R. Compound Semiconductors Strained Layers and Devices. Cham Heidelberg New York: Springer; 2000

[13] Hamelin A. In: Conway BE, White RE, O'M. Bockris J, editors. Modern Aspects of Electrochemistry. Vol. 16. New York: Plenum Press; 1985. p. 1

[14] Foresti ML, Pezzatini G, Cavallini M, Aloisi G, Innocenti M, Guidelli R. Electrochemical atomic layer epitaxy deposition of CdS on Ag(111): An electrochemical and STM investigation. The Journal of Physical Chemistry. B. 1998;**102**(38):7413-7420

[15] Carlà F, Loglio F, Resta A, Felici R, Lastraioli E, Innocenti M, Foresti ML. Electrochemical atomic layer deposition of CdS on Ag single crystals: Effects of substrate orientation on film structure. Journal of Physical Chemistry C. 2014;**118**:6132-6139

[16] Fernandes VC, Salvietti E, Loglio F, Lastraioli E, Innocenti M, Mascaro LH, Foresti ML. Electrodeposition of PbS multilayers on Ag(111) by ECALE. Journal of Applied Electrochemistry. 2009;**39**:2191-2197

[17] Innocenti M, Bencistà I, Bellandi S, Bianchini C, Di Benedetto F, Lavacchi A, Vizza F, Foresti ML. Electrochemical layer by layer growth and characterization of copper sulfur thin films on Ag(111). Electrochimica Acta. 2011;**58**:599-605

[18] Giaccherini A, Cinotti S, Guerri A, Carlà F, Montegrossi G, Vizza F, Lavacchi A, Felici R, Di Benedetto F, Innocenti M. Operando SXRD study of the structure and growth process of Cu2S ultra-thin films. Scientific Reports. 2017;**7**:1615

[19] Innocenti M, Bencista I, Di Benedetto F, Cinotti S, De Luca A, Bellandi S, Lavacchi A, Muniz Miranda M, Vizza F, Marinelli F, Dei L, Carretti E, Zafferoni C, Foresti ML. Underpotential deposition of Sn on S-covered Ag(111). ECS Transactions. 2013;**50**(21):1-7

[20] Hatchett DW, White HS. Electrochemistry of sulfur Adlayers on the low-index faces of silver. The Journal of Physical Chemistry. 1996;**100**(23):9854-9859

[21] Aloisi GD, Cavallini M, Innocenti M, Foresti ML, Pezzatini G, Guidelli R. In situ STM and electrochemical investigation of sulfur oxidative underpotential deposition on Ag(111). The Journal of Physical Chemistry. B. 1997;**101**(24):4774-4780

[22] Lastraioli E, Loglio F, Cavallini M, Simeone F, Innocenti M, Carlà F, Foresti ML. In situ scanning tunneling microscopy investigation of sulfur oxidative underpotential deposition on Ag(100) and Ag(110). Langmuir. 2010;**26**(22):17679-17685

[23] Perera AGU, Jayaweera PVV, Ariyawansa G, Matsik SG, Tennakone K, Buchanan M, Liu HC, Su XH, Bhattacharya P. Room temperature nano-and microstructure photon detectors. Microelectronics Journal. 2009;**40**(3):507-511

[24] Patil SV, Deshmukh PR, Lokhande CD. Fabrication and liquefied petroleum gas (LPG) sensing performance of p-polyaniline/n-PbS heterojunction at room temperature. Sensors and Actuators B: Chemical. 2011;**156**(1):450-455

[25] Brennan TP, Trejo O, Roelofs KE, Xu J, Prinz FB, Bent SF. Efficiency enhancement of solid-state PbS quantum dot-sensitized solar cells with Al_2O_3 barrier layer. Journal of Materials Chemistry A. 2013;**1**(26):7566-7571

[26] Lachenwitzer A, Morin S, Magnussen OM, Behm RJ. In situ STM study of electrodeposition and anodic dissolution of Ni on Ag(111). Physical Chemistry Chemical Physics. 2001;**3**(16):3351-3363

[27] Medway SL, Lucas CA, Kowal A, Nichols RJ, Johnson D. In situ studies of the oxidation of nickel electrodes in alkaline solution. Journal of Electroanalytical Chemistry. 2006;**587**(1): 172-181

[28] Innocenti M, Cattarin S, Cavallini M, Loglio F, Foresti ML. Characterisation of thin films of CdS deposited on Ag(111) by ECALE. A morphological and photoelectrochemical investigation. Journal of Electroanalytical Chemistry. 2002;**532**(1):219-225

[29] Cecconi T, Atrei A, Bardi U, Forni F, Innocenti M, Loglio F, Foresti ML, Rovida G. X-ray photoelectron diffraction (XPD) study of the atomic structure of the ultrathin CdS phase deposited on Ag(111) by electrochemical atomic layer epitaxy (ECALE). Journal of Electron Spectroscopy and Related Phenomena. 2001;**114-116**:563-568

[30] Blachnik R, Muller A. The formation of Cu_2S from the elements. II. Copper used in form of foils. Thermochimica Acta. 2001;**366**(1):47-59

[31] Beck Tan NC, Balogh L, Trevino SF, Tomalia DA, Lin JS. A small angle scattering study of dendrimer–copper sulfide nanocomposites. Polymer. 1999;**40**(10):2537-2545

[32] Bencista I, Di Benedetto F, Innocenti M, De Luca A, Fornaciai G, Lavacchi A, Montegrossi G, Oberhauser W, Pardi LA, Romanelli M, Vizza F, Foresti ML. Phase composition of Cu_xS thin films: Spectroscopic evidence of covellite formation. European Journal of Mineralogy. 2012;**24**:879-884

[33] Di Benedetto F, Bencistà I, Caporali S, Cinotti S, De Luca A, Lavacchi A, Vizza F, Muniz Miranda M, Foresti ML, Innocenti M. Electrodeposition of ternary $Cu_xSn_yS_z$ thin films for photovoltaic applications. Progress in Photovoltaics: Research and Applications. 2014;**22**: 97-106

[34] Di Benedetto F, Borrini D, Caneschi A, Fornaciai G, Innocenti M, Lavacchi A, Massa CA, Montegrossi G, Oberhauser W, Pardi LA, Romanelli M. Magnetic properties and cation ordering of nanopowders of the synthetic analogue of kuramite, Cu_3SnS_4. Physics and Chemistry of Minerals. 2011;**38**(6):483-490

[35] Innocenti M, Cattarin S, Loglio F, Cecconi T, Seravalli G, Foresti ML. Ternary cadmium and zinc sulfides: Composition, morphology and photoelectrochemistry. Electrochimica Acta. 2004;**49**:1327-1337

[36] Loglio F, Innocenti M, Pezzatini G, Foresti ML. Ternary cadmium and zinc sulfides and selenides: Electrodeposition by ECALE and electrochemical characterization. Journal of Electroanalytical Chemistry. 2004;**562**:117-125

[37] Caporali S, Tolstogouzov A, Teodoro OMND, Innocenti M, Di Benedetto F, Cinotti S, Picca RA, Sportelli MC, Cioffi N. Sn-deficiency in the electrodeposited ternary $Cu_xSn_yS_z$ thin films by ECALE. Solar Energy Materials & Solar Cells. 2015;**138**:9-16

[38] Di Benedetto F, Cinotti S, D'Acapito F, Vizza F, Foresti ML, Guerri A, Lavacchi A, Montegrossi G, Romanelli M, Cioffi N, Innocenti M. Electrodeposited semiconductors at room temperature: An X-ray absorption spectroscopy study of cu-, Zn-, S-bearing thin films. Electrochimica Acta. 2015;**179**:495-503

[39] Wei C, Myung N, Rajeshwar K. A combined voltammetry and electrochemical quartz crystal microgravimetry study of the reduction of aqueous Se(IV) at gold. Journal of Electroanalytical Chemistry. 1994;**375**:109-115

[40] Pezzatini G, Loglio F, Innocenti M, Foresti ML. Selenium(IV) electrochemistry on silver: A combined electrochemical quartz-crystal microbalance and cyclic voltammetric investigation. Collection of Czechoslovak Chemical Communications. 2003;**68**(9):1579-1595

[41] Cavallini M, Aloisi G, Guidelli R. An in situ STM study of selenium electrodeposition on Ag(111). Langmuir. 1999;**15**(8):2993-2995

[42] Russak MA, Reichman J, Witzke H, Deb SK, Chen SN. Thin film CdSe photoanodes for electrochemical photovoltaic cells. Journal of the Electrochemical Society. 1980;**127**(3): 725-733

[43] Liu C-HJ, Wang JH. Spray-pyrolyzed thin film CdSe photoelectrochemical cells. Journal of the Electrochemical Society. 1982;**129**(4):719-722

[44] Kim S, Fisher B, Eisler H-J, Bawendi M. Type-II quantum dots: CdTe/CdSe(core/shell) and CdSe/ZnTe(core/shell) heterostructures. Journal of the American Chemical Society. 2003; **125**(38):11466-11467

[45] Dabbousi BO, Rodriguez-Viejo J, Mikulec FV, Heine JR, Mattoussi H, Ober R, Jensen KF, Bawendi MG. (CdSe)ZnS core−shell quantum dots: Synthesis and characterization of a size series of highly luminescent Nanocrystallites. The Journal of Physical Chemistry B. 1997;**101**(46):9463-9475

[46] Gur I, Fromer NA, Geier ML, Alivisatos AP. Air-stable all-inorganic nanocrystal solar cells processed from solution. Science. 2005;**310**(5747):462-465

[47] Huang Y, Duan X, Lieber CM. Nanowires for integrated multicolor nanophotonics. Small. 2005;**1**(1):142-147

[48] Loglio F, Innocenti M, D'acapito F, Felici R, Pezzatini G, Salvietti E, Foresti ML. Cadmium selenide electrodeposited by ECALE: Electrochemical characterization and preliminary results by EXAFS. Journal of Electroanalytical Chemistry. 2005;**575**(1):161-167

[49] Pezzatini G, Caporali S, Innocenti M, Foresti ML. Formation of ZnSe on Ag(111) by electrochemical atomic layer epitaxy. Journal of Electroanalytical Chemistry. 1999;**475**(2): 164-170

[50] Loglio F, Telford AM, Salvietti E, Innocenti M, Pezzatini G, Cammelli S, D'Acapito F, Felici R, Pozzi A, Foresti ML. Ternary $Cd_xZn_{1-x}Se$ deposited on Ag (111) by ECALE: Electrochemical and EXAFS characterization. Electrochimica Acta. 2008;**53**:6978-6987

[51] Mori E, Baker CK, Reynolds JR, Rajeshwar K. Aqueous electrochemistry of tellurium at glassy carbon and gold: A combined voltammetry-oscillating quartz crystal microgravimetry study. Journal of Electroanalytical Chemistry. 1988;**253**:441-451

[52] Traore M, Modolo R, Vittori O. Electrochemical behaviour of tellurium and silver telluride at rotating glassy carbon electrode. Electrochimica Acta. 1988;**33**:991-996

[53] Forni F, Innocenti M, Pezzatini G, Foresti ML. Electrochemical aspects of CdTe growth on the face (111) of silver by ECALE. Electrochimica Acta. 2000;**45**:3225-3231

[54] Liang YQ, Zhai L, Zhao XS, Xu DS. Band-gap engineering of semiconductor nanowires through composition modulation. The Journal of Physical Chemistry B. 2005;**109**(15): 7120-7123

[55] Takahashi T, Nichols P, Takei K, Ford AC, Jamshidi A, Wu MC, Ning CZ, Javey A. Contact printing of compositionally graded CdS_xSe_{1-x} nanowire parallel arrays for tunable photodetectors. Nanotechnology. 2012;**23**(4):045201

[56] Foresti ML, Milani S, Loglio F, Innocenti M, Pezzatini G, Cattarin S. Ternary $CdS_xSe_{(1-x)}$ deposited on Ag(111) by ECALE: Synthesis and characterization. Langmuir. 2005;**21**(15): 6900-6907